Annals of Biomedical Engineering (© 2012)
DOI: 10.1007/s10439-012-0573-9

BMES BIOMEDICAL ENGINEERING SOCIETY™ www.bmes.org

Ultrasound Imaging of Oxidative Stress *In Vivo* with Chemically-Generated Gas Microbubbles

JOHN KANGCHUN PERNG,[1] SEUNGJUN LEE,[1] KOUSIK KUNDU,[1] CHARLES F. CASKEY,[2] SARAH F. KNIGHT,[3] SARP SATIR,[4] KATHERINE W. FERRARA,[2] W. ROBERT TAYLOR,[3,5] F. LEVENT DEGERTEKIN,[4] DANIEL SORESCU,[3] and NIREN MURTHY[1]

[1]The Wallace H. Coulter Department of Biomedical Engineering, Parker H. Petit Institute for Bioengineering and Bioscience, Georgia Institute of Technology, 315 Ferst Drive, Atlanta, GA 30332, USA; [2]Department of Biomedical Engineering, University of California—Davis, Davis, CA 95616, USA; [3]Cardiology Division, School of Medicine, Emory University, Atlanta, GA 30322, USA; [4]School of Mechanical Engineering, Georgia Institute of Technology, Atlanta, GA 30332, USA; and [5]Atlanta VA Medical Center, Atlanta, GA 30322, USA

(*Received 7 August 2011; accepted 11 April 2012*)

Associate Editor James Tunnell oversaw the review of this article.

Abstract—Ultrasound contrast agents (UCAs) have tremendous potential for *in vivo* molecular imaging because of their high sensitivity. However, the diagnostic potential of UCAs has been difficult to exploit because current UCAs are based on pre-formed microbubbles, which can only detect cell surface receptors. Here, we demonstrate that chemical reactions that generate gas forming molecules can be used to perform molecular imaging by ultrasound *in vivo*. This new approach was demonstrated by imaging reactive oxygen species *in vivo* with allylhydrazine, a liquid compound that is converted into nitrogen and propylene gas after reacting with radical oxidants. We demonstrate that allylhydrazine encapsulated within liposomes can detect a 10 micromolar concentration of radical oxidants by ultrasound, and can image oxidative stress in mice, induced by lipopolysaccharide, using a clinical ultrasound system. We anticipate numerous applications of chemically-generated microbubbles for molecular imaging by ultrasound, given ultrasound's ability to detect small increments above the gas saturation limit, its spatial resolution and widespread clinical use.

Keywords—Ultrasound contrast agent, Molecular imaging, Reactive oxygen species (ROS), Oxidative stress, Bubble nucleation, Chemical gas generation.

INTRODUCTION

Current UCAs for molecular imaging are composed of pre-formed gas bubbles conjugated with ligands, which bind to cell surface receptors and have been used with great success for imaging angiogenesis,[39] activated leukocytes[12,30] and thrombus.[26] However, current UCAs image only cell surface receptors and numerous disease biomarkers are not expressed on the cell surface. For example, radical oxidants are disease biomarkers that are central to the development of numerous inflammatory diseases,[18] such as cardiovascular[20] and neuro-degenerative diseases,[2] and cannot be imaged with ligand-receptor interactions. Currently there are no ultrasound contrast agents that can image radical oxidants in a clinical setting.

In this report, we demonstrate that radical oxidants can be imaged by ultrasound *via* chemical reactions that generate gas bubbles in the presence of radical oxidants. This strategy is shown in Fig. 1, and is based on a new contrast agent composed of allylhydrazine encapsulated within phospholipid liposomes (termed APLs). Allylhydrazine (**1**) is the ROS sensitive component of the APLs and oxidizes into 2-propenyl-diazene (**2**) in the presence of radical oxidants. 2-Propenyl-diazene is an unstable intermediate and spontaneously undergoes a retro-ene reaction to generate the gas forming molecules nitrogen and propene (**3**).[23,32] The APLs are designed to generate gas forming molecules in tissue that over-produce radical oxidants, and therefore change the acoustic impedance of tissue experiencing oxidative stress, making it detectable by ultrasound. The limit for detecting gas molecules above saturation in aqueous solutions by ultrasound is a key parameter determining the feasibility of using the APLs for ROS imaging. We demonstrate here that ultrasound can detect a 1–2% increase in nitrogen gas concentration above saturation, generated from the reaction of APLs

Address correspondence to Niren Murthy, The Wallace H. Coulter Department of Biomedical Engineering, Parker H. Petit Institute for Bioengineering and Bioscience, Georgia Institute of Technology, 315 Ferst Drive, Atlanta, GA 30332, USA. Electronic mail: nmurthy@berkeley.edu

© 2012 Biomedical Engineering Society

Published online: 05 May 2012

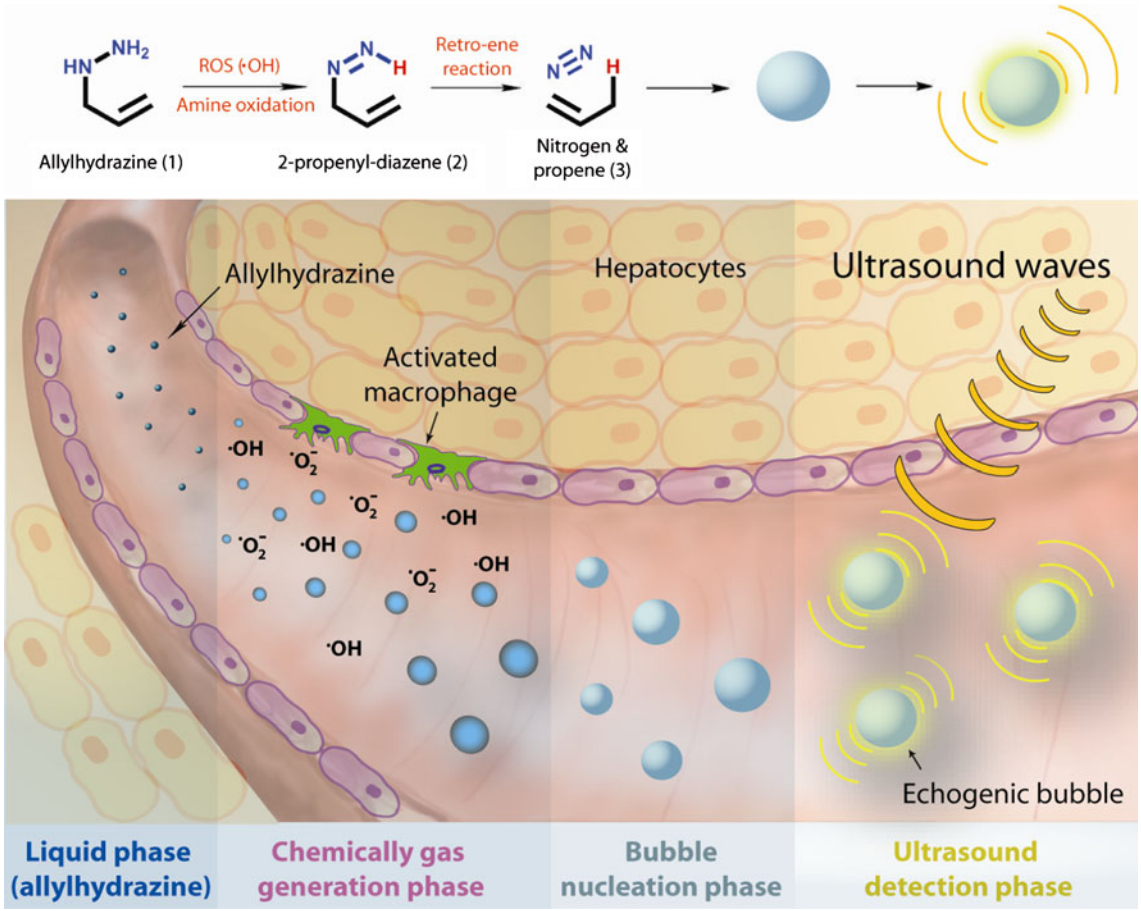

FIGURE 1. Chemically generated microbubbles—a new strategy to image oxidative stress *in vivo* by ultrasound. Allylhydrazine (1) undergoes a liquid to gas phase transition in the presence of radical oxidants. Allylhydrazine is oxidized by radical oxidants through an amine oxidation reaction, forming 2-propenyl-diazene (2), which is an unstable intermediate that generates nitrogen and propene gas molecules (3) *via* an intramolecular retro-ene reaction. The increase in gas concentration results in a change in acoustic impedance that can be detected acoustically. For *in vivo* imaging, allylhydrazine encapsulated within phospholipid liposomes (APLs) are injected intravenously and increase echo intensity in tissues that overproduce radical oxidants by nucleating gas bubbles. Relative oxidative stress can be detected by scanning the region of interest with ultrasound and measuring the change in video intensity.

with radical oxidants, resulting in a 10 μM detection limit for the hydroxyl radical. Finally, we show that the APLs can image oxidative stress *in vivo via* ultrasound in the liver of mice in a lipopolysaccharide (LPS) model of inflammation.[28]

MATERIALS AND METHODS

Oxidation Kinetics of Allylhydrazine Determined with the ABTS Assay

A stock solution of the 2,2′-azinobis-3-ethylbenzothiazoline-6-sulfonic acid (ABTS, Sigma-Aldrich, USA) radical cation was prepared by adding 1 mL of sodium persulfate (68.9 mM) to 99 mL of ABTS solution (5 mM) in PBS (pH 8.0). The mixture was stored in the dark for 16 h to generate ABTS radicals, which gave an absorbance at 734 nm. The stock solution of ABTS (1 mL, 689 μM) was added to allylhydrazine (2 mL, pH 7.0, 10 mM) and the absorbance at 734 nm was measured using a UV–VIS spectrophotometer (UV-1700, Shimadzu). The pseudo first-order oxidation kinetics and the half-life were determined by curve fitting.

Optical and Acoustic Observation of Bubble Nucleation with Allylhydrazine

A custom-built optical and acoustic measuring system was developed that can simultaneously visualize bubble nucleation and characterize its acoustic properties. A solution containing 100 mM allylhydrazine and 1 mM hydroxyl radical (H_2O_2 + Fe^{2+}) was premixed in a syringe and injected into a 200 μm-diameter cellulose tube at a controlled flow rate. The tube was placed at the focal depth of a focused transducer, and interrogated with 1.5 pulse cycles at a 2.25 MHz center

frequency with an 80 Hz PRF. The cellulose tube was placed under a microscope stage linked to a digital camera for optical observation of bubble nucleation. The acoustic data was acquired with an oscilloscope and processed off-line by a computer.

In Vitro Acoustic Detection of the Hydroxyl Radical with Allylhydrazine

A second custom-built ultrasound measuring system was constructed to quantify the ability of allylhydrazine to detect the hydroxyl radical. Free allylhydrazine or APLs were injected into an acoustically-transparent holder, kept at 37 °C, and placed at the near-field boundary of an unfocused transducer. A 2.25 MHz single element unfocused transducer (IS0204HR, Valpey Fisher) with a 0.5″ element diameter and a near-field boundary of 6 cm was used to generate ultrasound pulse sequences (2.05 MHz center frequency, 0.6 MPa pressure, 20 pulse cycles and 100 Hz PRF), using an Agilent HP32250A arbitrary waveform generator, and were amplified through an ENI 320L RF power amplifier. The acoustic intensity of the allylhydrazine solution was measured before and after various concentrations of the hydroxyl radical (Fe^{2+} and H_2O_2) were added, and the fold increase was calculated by dividing the acoustic intensity prior to the addition of the hydroxyl radical. The acoustic echo from the holder containing allylhydrazine and the hydroxyl radical was detected using a calibrated hydrophone (HGL-1000, Onda Corporation) with a 20 dB gain preamplifier (AH-2010, Onda Corporation). The received signal was recorded on a HP DSO5014A digital oscilloscope and Fast Fourier Transform (FFT) signal processing was performed using a MATLAB interface.

Encapsulation of Allylhydrazine Within Liposomes

Allylhydrazine was encapsulated into phospholipid liposomes to enhance its *in vivo* efficacy. The liposomes were composed of 80 mol% distearoylphosphatidylcholine (DSPC), 10 mol% dipalmitoylphosphatidic acid (DPPA), and 10 mol% *N*-(carbonyl-methoxypolyethyleneglycol 5000) dipalmitoylphosphoethanolamine (DPPE-PEG5000) purchased from Genzyme (Pittsburgh, PA). Briefly, 100 mg of lipid were dissolved in chloroform and placed in a round bottom flask, the solvent was evaporated on a rotovap, forming a thin film, which was vacuum dried overnight. The lipid film was reconstituted with an allylhydrazine solution (1 M) to reach a final lipid concentration of 10 mg mL^{-1}, and heated to 5 °C above the phospholipid phase transition temperature (T_m = 55 °C for DSPC), followed by rapid quenching at 0 °C in an ice-water bath. The heating/cooling cycle was repeated 3–5 times until a clear/semi-transparent solution was observed.[22,27,29] The liposomes were dialyzed with a 2000 Da MWCO dialysis membrane for 6 h (Pierce Slide-A-Lyzer dialysis cassettes, Thermo Scientific), and the size distribution was determined with a Particle Size Analyzer (90-Plus, Brookhaven Instruments Corporation). The amount of allylhydrazine encapsulated within the liposomes was determined using the TNBS assay.

Determination of Encapsulation Efficiency with Trinitrobenzene Sulfonic Acid (TNBS) Assay

Briefly, allylhydrazine was encapsulated within liposomes using the methods described in the liposome preparation section. A portion of the allylhydrazine-encapsulated liposome solution was dialyzed with a 2000 Da MWCO dialysis membrane for 6 h. Both dialyzed and undialyzed liposomes were lysed with 3% Triton to release the free allylhydrazine, and subjected to the TNBS assay.[25,36]

The liposome solution (1 mL) was added to 1 mL of 4% $NaHCO_3$ (pH 8.5), and the mixture was incubated in a water bath at 42 °C for 10 min. Next, 1 mL of 0.01% (341 μM) freshly made TNBS was added to the mixture and incubated at 42 °C for 2 h followed by the addition of 1 mL 10% SDS and 0.5 mL of 1 N HCl. The absorbance was monitored at 335 nm, after appropriate blank corrections. The blank correction is prepared by the same procedure except that concentrated HCl was added to the allylhydrazine solution prior to the addition of the TNBS reagent. To determine the encapsulation efficiency, the undialyzed liposome solution was subjected to TNBS assay described above. The encapsulation efficiency of allylhydrazine inside liposomes was determined by the TNBS assay to be 5.2%.

Biodistribution of APL-Based Liposomes In Vivo

Rhodamine was encapsulated into phospholipid liposomes composed of 80 mol% DSPC, 10 mol% DPPA, and 10 mol% DPPE-PEG5000 purchased from Genzyme (Pittsburgh, PA). Briefly, 50 mg of lipid were dissolved in chloroform and placed in a round bottom flask, the solvent was evaporated on a rotovap, forming a thin film, which was vacuum dried overnight. Rhodamine B solution (4.2 mM) was added to 50 mg liposomes to reach a 10 mg mL^{-1} lipid concentration. The liposome solution was heated to 55 °C, followed by rapid quenching at 0 °C in an ice-water bath. The heating/cooling cycle was repeated 3–5 times until a clear/semi-transparent solution is observed. The liposomes solution was separated into two vials; one vial contained undialyzed liposomes, and the other half was dialyzed with a 2000 Da MWCO dialysis membrane for 16 h

(Pierce Slide-A-Lyzer dialysis cassettes, Thermo Scientific). Both dialyzed and undialyzed liposomes were lysed with 3% Triton, and the fluorescence was measured with a plate reader using filter settings for Rhodamine B (Ex: 540/Em: 625). The encapsulation efficiency was determined by dividing the fluorescence of dialyzed solution over undialyzed solution. The encapsulation efficiency of Rhodamine B inside liposome was determined to be 4.2%. APL-based liposomes loaded with Rhodamine B dye were injected intravenously into mice ($n = 3$), the mice were killed after 10 min and the biodistribution of the liposomes was determined. The organs were isolated and weighed. Briefly, 100 mg of tissue was homogenized in 1 mL of cell-lysis RIPA buffer (Cell Signaling Technology, Danvers, MA) and sonicated to ensure full disruption of tissue. The homogenate was centrifuged for 2.5 min at 9000 rpm and the supernatant was aliquoted into a microplate, and the fluorescence was measured using filter settings for Rhodamine B (Ex: 540/Em: 625). The fluorescence was normalized to the tissue weight and plotted after subtracting background auto-fluorescence, determined by injecting empty liposomes into control mice ($n = 3$).

In Vivo Ultrasound Imaging of LPS-Induced Oxidative Stress in Mice with Allylhydrazine-Based Contrast Agents

Two groups of C57Bl/6 male mice ($n = 5$ per group), aged 8–10 weeks, were obtained from Jackson Labs. Inflammation was induced by injecting 200 μL of LPS in saline (2 mg mL^{-1}) into the peritoneal cavity of the mice, 200 μL of saline was injected into control mice. 20 h later the mice were anaesthetized with isofluorane and the fur on the chest and abdomen was removed. An ultrasound probe was placed horizontally across the ventral surface of the mice chest, and 100 μL of APLs solution (14 mg allylhydrazine per mouse) was injected intravenously into the retro-orbital venous sinus. The mouse liver was imaged using a 14 MHz Siemens Acuson Sequoia 512 clinical ultrasound system (Siemens, USA) for 10 min after allylhydrazine injection. The image settings for the clinical ultrasound system are MI = 0.05, 187 kPa pressure, 1.5 pulse cycles and 70 Hz pulse repetition frequency, T1 space–time, +1 edge, 0 persistence, 4 post-processing and a delta of 2. A gray scale mapping function was used to calibrate the ultrasound video intensity to ensure the video image results were in the linear region. DICOM image data were processed with ImageJ software (NIH). The mean video intensity in the ROI (the liver) was analyzed and normalized by dividing the video intensity at any given time point by the video intensity at the time of contrast agent injection (time = 0). All animal studies were conducted under a protocol that was approved by the Animal Use and Care Committee of Emory University.

Statistical Evaluation

All treatment groups were analyzed for statistical significance (*$p < 0.05$) by an unpaired t-test. The data were expressed as means ± SE with a sample size of 4 for *in vitro* ultrasound characterization (Figs. 2d and 3a–3c). For *in vivo* studies, the data were expressed as means ± SE with a sample size of 5 (Fig. 4c). A value of $p < 0.05$ was considered statistically significant.

RESULTS

Oxidation Kinetics of Allylhydrazine

The APLs are designed to nucleate gas bubbles in the presence of radical oxidants. In order to exceed the critical threshold needed for bubble nucleation, the allylhydrazine in the APLs needs to oxidize rapidly in comparison to the rate of nitrogen diffusion. We therefore investigated the oxidation kinetics of allylhydrazine with 2,2′-azino-bis-3-ethylbenzothiazoline-6-sulfonic acid (ABTS), a radical cation that is reduced by single electron oxidation of its substrates.[33] Figure 2a demonstrates that allylhydrazine (6.6 mM) was rapidly oxidized by ABTS (230 μM), with a half-life of 3.06 s and a pseudo first-order rate constant (k) of 0.23 s^{-1}, which is consistent with literature values.[9] This suggests that allylhydrazine has the reactivity needed to nucleate bubbles *in vivo*.

In Vitro Acoustic Characterization and Optical Observation of Bubble Nucleation

We examined if the oxidation of allylhydrazine by the hydroxyl radical could chemically generate gas bubbles, using a custom-built system that simultaneously visualizes gas bubbles and measures their acoustic properties. For these experiments, a 100 mM allylhydrazine solution containing a 1 mM hydroxyl radical concentration (Fenton's reagent) was injected into a 200 μm-diameter cellulose tube and then imaged. Figure 2b demonstrates that allylhydrazine can nucleate bubbles in the presence of hydroxyl radicals. Figure 2b1 shows an image of the cellulose tube containing deionized water, and has no evidence of bubble formation. In contrast, after injecting allylhydrazine and Fenton's reagent into the cellulose tube, bubbles became optically visible. For example, Fig. 2b2–4 shows a bubble flowing through the cellulose tube generated from the oxidation of allylhydrazine with the hydroxyl radical. We further investigated if the gas bubbles generated from the oxi-

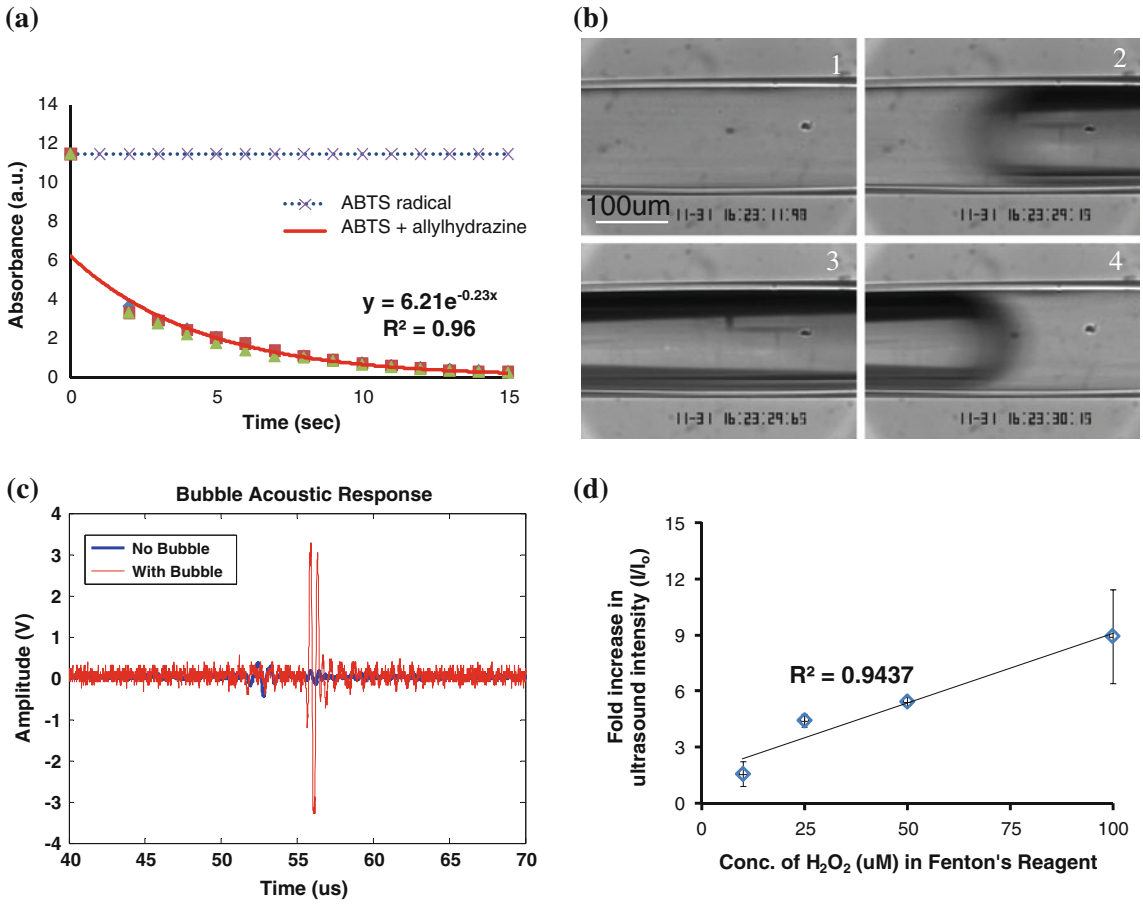

FIGURE 2. Allylhydrazine can detect radical oxidants and nucleate gas bubbles in the presence of radical oxidants. (a) Allylhydrazine reacts rapidly with radical oxidants. ABTS radical cation has a constant absorbance at 734 nm (dash line). ABTS radical cation (230 μM) is reduced by excess allylhydrazine (6.6 mM) and loses its absorbance (red curve), with a pseudo first-order kinetic rate constant of 0.23 s^{-1} (n = 3). (b) Allylhydrazine can nucleate gas bubbles in the presence of the hydroxyl radical. A 200 μm-diameter cellulose tube was placed under a microscope with a camera in an acoustic measuring system. A solution containing 100 mM allylhydrazine and 1 mM hydroxyl radical was injected into the tube. There was no evidence of bubble formation inside the cellulose tube prior to the hydroxyl radical injection (1). After the injection, gas bubbles became visible inside the cellulose tube, and video images (2–4) demonstrate a single gas bubble flowing through the cellulose tube. (c) The microbubble identified by optical observation in 2c generates a strong acoustic echo (55–58 μs). The microbubble displays a 20-fold increase in acoustic signal intensity compared to adjacent fluid. (d) Allylhydrazine can detect a 10 μM hydroxyl radical concentration and displays a linear correlation between ultrasound intensity and the hydroxyl radical concentrations within the range of 10–100 μM (R^2 = 0.94, the hydroxyl radical was generated by H_2O_2 + Fe^{2+}). Allylhydrazine (100 mM) was mixed with various concentrations of the hydroxyl radical, and the acoustic response was measured 10 min later using a custom-built acoustic measuring system. The fold increase in ultrasound intensity was calculated by dividing the acoustic intensity with radical oxidants (I) by the acoustic intensity prior to the addition of radical oxidants (I_o). The vertical bars represent standard error with a sample size of 4 for each data point.

dation of allylhydrazine by the hydroxyl radical could be detected acoustically. Figure 2c demonstrates that strong acoustic echoes are generated from a microbubble identified by optical observation (55–58 μs). For example, the microbubble identified in Fig. 2b2–4 displayed a 20-fold increase in acoustic signal intensity in comparison to adjacent fluid at 2.25 MHz frequency using a 0.5″ diameter transducer at a distance of 5.1 cm. Chemically generated gas bubbles were also observed at lower hydroxyl radical concentrations (100 μM), albeit at a slower rate.

Physiologic radical oxidants concentrations are speculated to occur in the nanomolar to micromolar range,[8] and we investigated if allylhydrazine could detect radical oxidants at this low concentration. Excess allylhydrazine (100 mM) was mixed with various concentrations of the hydroxyl radical (10–100 μM) and the ultrasound echo response was transmitted and received at 2.25 MHz (Mechanical Index = 0.28). All echo responses were recorded over 15 min and the ultrasound signal reached its peak intensity after 10 min and remained saturated for at least 5 more minutes. Therefore, the ultrasound intensity at the 10 min time-point was chosen for comparison between various concentrations of the hydroxyl radical. Figure 2d demonstrates that allylhydrazine can detect a

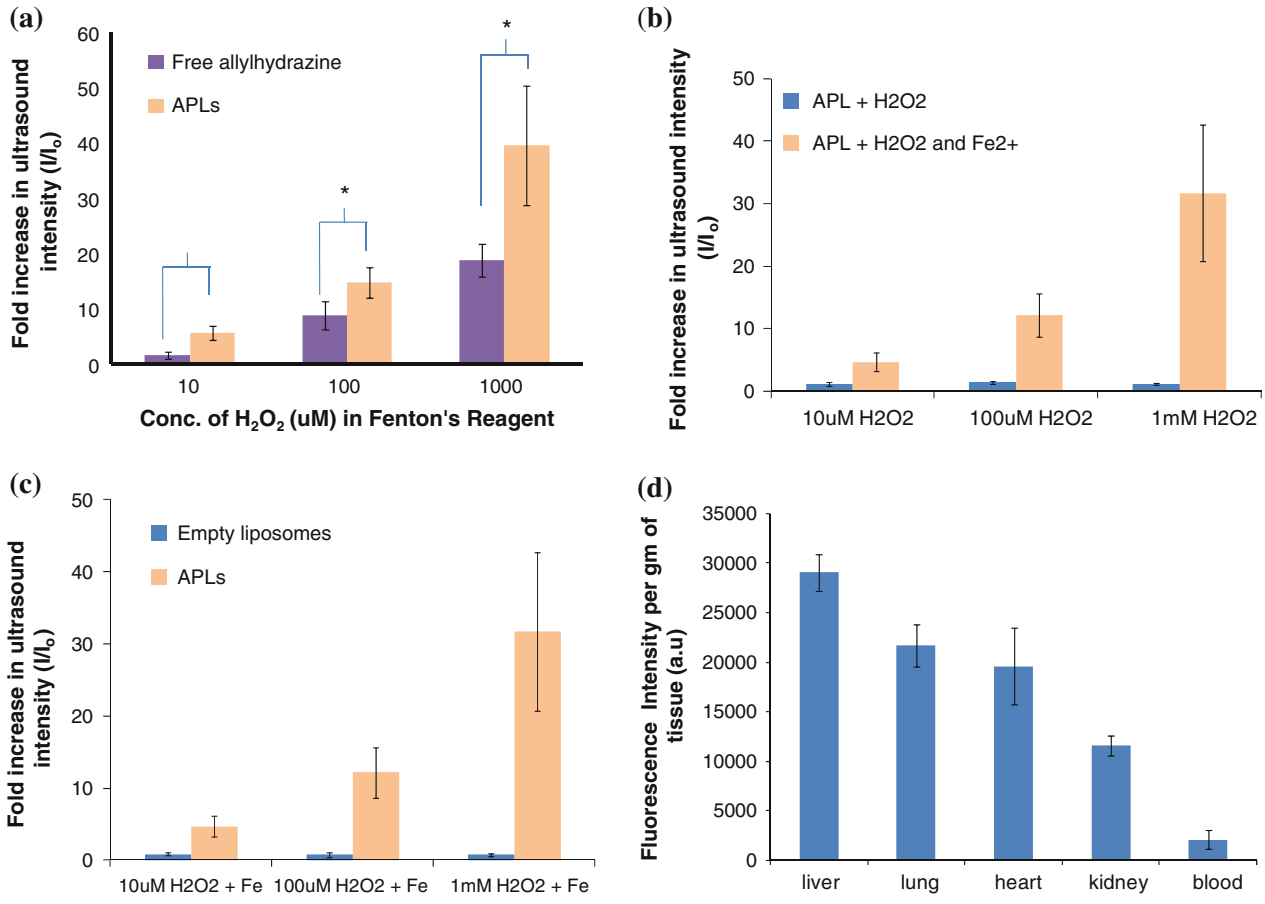

FIGURE 3. Liposome encapsulation of allylhydrazine can improve bubble stability and *in vivo* delivery. (a) The APLs have greater sensitivity to radical oxidants than free allylhydrazine. The APLs were mixed with various concentrations of the hydroxyl radical, and the acoustic response was measured 10 min later using a custom-built acoustic measuring system. The vertical bars represent standard error with a sample size of 4 for each data point. (b) The specificity of the APLs toward the hydroxyl radical was investigated. The APLs (100 mM) were mixed with various H_2O_2 concentrations (10 μM, 100 μM, 1 mM) with and without Fe^{2+}. The relative ultrasound intensity did not increase with H_2O_2, however, did with H_2O_2 + Fe^{2+}. (c) Empty liposomes do not increase their ultrasound intensity in response to radical oxidants. Empty liposomes with the same compositions as the APLs (but without allylhydrazine) were investigated with various concentrations of H_2O_2 and Fe^{2+} (1 mM). No increase in ultrasound intensity was observed, confirming that liposomes alone do not contribute to the increased ultrasound echogenicity of the APLs. Comparison of empty liposomes versus liposomes loaded with allylhydrazine demonstrated that allylhydrazine is the source of ultrasound signal in bubble generation. (d) APL-based liposomes loaded with Rhodamine B dye reach the liver within 10 min. APL-based liposomes loaded with Rhodamine B dye were injected intravenously into mice (n = 3), the mice were killed after 10 min and the organs were isolated to determine the biodistribution of the liposomes. The liposomes accumulated predominantly in the liver and lung.

10 μM hydroxyl radical concentration, and displays a linear correlation between ultrasound intensity and hydroxyl radical concentrations within the range of 10–100 μM ($R^2 = 0.94$).

Liposome Encapsulation of Allylhydrazine

Allylhydrazine was encapsulated into phospholipid liposomes (APLs) with a size distribution ranging from 60 to 110 nm in diameter. Liposomes can enhance bubble nucleation from allylhydrazine and reduce bubble dissolution by decreasing the surface tension at the gas–liquid interface.[5,7] Another key advantage of liposomal delivery is its efficient loading and that large amount of allylhydrazine can be delivered locally, thus minimizing dilution during the transport. We examined if the APLs would produce a stronger acoustic signal in response to radical oxidants than free allylhydrazine *in vitro*. Figure 3a shows that APLs are more effective at detecting the hydroxyl radical than free allylhydrazine. For example, for a 10 μM hydroxyl radical concentration the ultrasound intensity of the

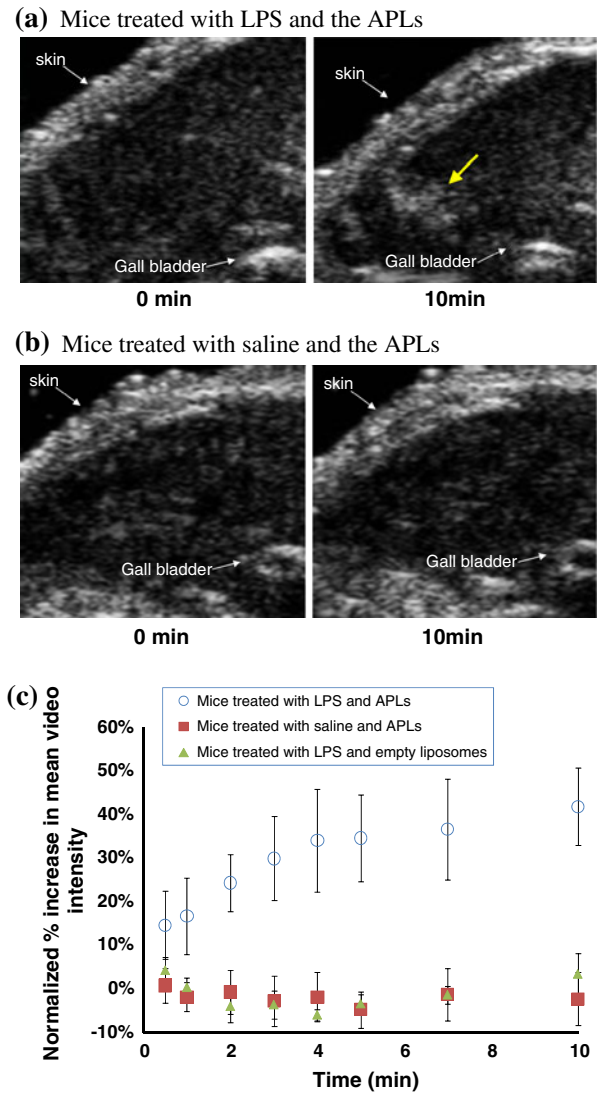

FIGURE 4. The APLs can enhance acoustic contrast and image oxidative stress *in vivo* during a LPS-induced inflammatory response. (a) LPS (0.4 mg per mouse) was injected into the peritoneal cavity of mice ($n = 5$), 20 h later the APLs (14 mg allylhydrazine per mouse) were injected intravenously. Representative ultrasound images of the mouse liver show enhanced acoustic contrast 10 min after the APLs injection. Arrow indicates location of enhanced acoustic contrast in the liver. (b) Saline was injected into the peritoneal cavity of control mice ($n = 5$), 20 h later the APLs (14 mg allylhydrazine per mouse) were injected intravenously. Representative ultrasound images of the mouse liver did not show significant changes 10 min after the APLs injection. (c) Quantitative image analysis of the ultrasound images in (a) and (b) demonstrates that mice treated with the APLs and LPS increased their normalized mean video intensity by 40% (circles), compared to no increase in control mice treated with the APLs and saline (squares). The mean video intensity was normalized to the video intensity at the time of injection. In addition, quantitative image analysis of mice treated with LPS and empty liposomes ($n = 5$) did not show an increase in normalized mean video intensity (triangles). The vertical bars represent standard error.

APLs increased 5.6-fold compared to only 1.6-fold for free allylhydrazine. Additional controls were performed and Fig. 3b demonstrates that the APLs are specific for the hydroxyl radical. For example, adding hydrogen peroxide alone to the APLs did not produce significant ultrasound signals, but adding the hydroxyl radical generated from Fenton's reagent ($H_2O_2 + Fe^{2+}$) to the APLs resulted in strong ultrasound signals within 10 min which were concentration dependent. This *in vitro* result also shows that the hydroxyl radical can diffuse into the liposome and react with the allylhydrazine inside the liposome. To further verify that the ultrasound signals are not the result of echogenic liposomes, Fig. 3c shows that empty liposomes do not increase ultrasound intensity in response to radical oxidants. We also examined the effect of PEGylation on liposomes, and we found that liposomes without PEGylation are not as effective as PEGylated liposomes at detecting ROS *in vitro* (data not shown). Lastly, we investigated the *in vivo* biodistribution of APL-based liposomes and Fig. 3d verifies that the liposome formulation used to generate the APLs was capable of reaching the liver within 10 min. Therefore, the APLs have the potential to improve the ability of allylhydrazine to detect radical oxidants *in vivo*.

In Vivo Ultrasound Imaging of Oxidative Stress with APLs

We investigated the *in vivo* feasibility of using APLs to image oxidative stress in mice, triggered by an LPS-induced inflammatory response.[28] Mice were given an intraperitoneal injection of LPS, or saline as a control, and the APLs (14 mg allylhydrazine per mouse) were injected intravenously into the retro-orbital venous sinus 20 h later. The mice were imaged with a Siemens Acuson clinical ultrasound system at a 14 MHz frequency. Figure 4a illustrates that APLs can enhance acoustic contrast in mice experiencing oxidative stress while maintaining a low background signal in healthy mice. For example, 10 min after the APL injection, several bright spots became visible in the livers of LPS-treated mice, but not in mice treated with saline (Fig. 4b). We performed quantitative analysis on the ultrasound images and Fig. 4c shows that after 10 min, the normalized mean video intensity of LPS-treated mice increased by 40%, but remained at baseline intensity levels for mice treated with saline. We also verified that the injection of empty APL-based liposomes (at the same lipid concentration used in Fig. 4a) into LPS-treated mice ($n = 5$) did not produce enhanced ultrasound echoes, demonstrating that

inflammation in tissue alone does not enhance ultrasound echoes. Together, these results demonstrate that the APLs can detect oxidative stress *in vivo* with excellent spatial and contrast resolution that cannot be achieved using fluorescent[21] or chemiluminescent[10] based contrast agents.

DISCUSSIONS

The overproduction of reactive oxygen species is associated with numerous diseases, and the ability to detect oxidative stress *in vivo* in a clinical setting has the potential to significantly improve the diagnosis of human disease. Hence, the development of ultrasound imaging methods that can detect ROS can have a great impact on translational medicine. This work presents a new approach to perform ultrasound imaging of oxidative stress *in vivo via* chemical reactions that generate gas forming molecules in the presence of ROS. The concept of generating gases inside liposomes *via* chemical reactions has been described in the patent literature using liposomes containing gas precursors such as carbonate and bicarbonates.[35,38] The key issues for this strategy to be successful are: (1) the kinetics of gas generation should be faster than gas diffusion for bubbles to nucleate, (2) the sensitivity of ultrasound to detect gas formation from chemical reactions, and (3) translating this approach into more complex and dynamic conditions *in vivo*.

A key requirement for bubble nucleation is that the rate of nitrogen gas generated by allylhydrazine should be substantially faster than the rate of nitrogen gas diffusion in ROS-producing tissue. We chose allylhydrazine as the ROS-sensitive component of the APLs because of the extensive literature demonstrating that the amine oxidation of hydrazine-based molecules is rapid. For example, Calderwood *et al.* demonstrated that substituted hydrazines can be oxidized rapidly by superoxide ion ($O_2^{-\bullet}$) with a half-life of 0.43 s.[9] In addition, Corey *et al.* showed that allylic hydrazine can be oxidized by radicals through an amine oxidation reaction, followed by a 1,5-sigmatropic rearrangement of hydrogen with loss of nitrogen gas.[14] Therefore, we anticipated that allylhydrazine would be oxidized by free radicals through an amine oxidation, and then undergo an intramolecular retro-ene reaction to form nitrogen and propene gas molecules. To evaluate the feasibility of this chemical reaction, the Thiele modulus of the oxidation of allylhydrazine with the hydroxyl radical was calculated,[3] assuming a 1 mm length of ROS over-producing tissue, a nitrogen diffusion constant of 2.83×10^{-5} cm^2 s^{-1},[17] and a rate constant k of 0.23 s^{-1} obtained from Fig. 2a, the Thiele modulus for this system was determined to be 9. A Thieles modulus value greater than one indicates that the rate of reaction is faster than the rate of diffusion, suggesting that allylhydrazine has the reactivity needed to nucleate bubbles *in vivo*.

Physiological concentrations of ROS are believed to occur in the nanomolar to micromolar range, and detecting this low level of radical oxidants can be challenging because classical bubble nucleation theory predicts that homogenous bubble nucleation occurs only at concentrations significantly above gas supersaturation.[4,24] For example, classical bubble nucleation theory predicts that nitrogen gas bubbles will only nucleate at concentrations above 5 mM (assuming homogenous nucleation). To address the issue of bubble nucleation, many have shown that in the presence of pre-existing bubble nuclei, such as on the surfaces of the container or in the bulk solution, bubble nucleation occurs at much lower concentrations than theoretical prediction.[24,31] These bubble nuclei or 'embryos' enhance bubble nucleation by lowering the energy barrier required to reach the critical nuclei radius.[4,19] It has also been reported that bubble nucleation generated from chemical reactions occurs at much lower concentrations than theoretical prediction.[6] These reports suggest that although classical bubble nucleation theory is useful in predicting homogenous bubble nucleation, it has limited applications in heterogeneous conditions.[31]

Few studies have evaluated supersaturated fluids, and our *in vitro* studies showed that ultrasound is able to detect a 10 μM radical oxidant concentration (Fig. 2d), which represents a small increase above the nitrogen gas saturation concentration (450 μM). The pressure threshold for ultrasonically-induced nucleation in homogeneous pure water has been reported to exceed 100 MPa.[41] With the presence of gas nuclei in homogeneous water, the cavitation threshold is ~0.5 MPa at 0.75 or 1 MHz,[1] and with the inclusion of physiologically-relevant nuclei, gas saturation and interfacial tension, the threshold for ultrasonically-induced nucleation decreases to several hundred kilopascal at 1 MHz.[13] Peak acoustic pressure normalized by the square root of frequency is a commonly applied metric for the likelihood of cavitation—in these studies this metric was less than 0.42 and therefore was below the pressure typically associated with cavitation. Here, nitrogen gas bubbles were generated in the presence of ROS, increasing gas saturation beyond the saturation limit and thus creating a state in which small perturbations are expected to result in bubble nucleation. We hypothesize that the perturbations induced by ultrasound, as applied here, could enhance the nucleation rate and thereafter bubble growth. We also speculate that we are detecting mixed states of gas and liquid by ultrasound, because of the low radical oxidant con-

centrations and relatively low ultrasound pressure used here.[34] In addition, perturbations induced by ultrasound as applied here could enhance the nucleation rate and bubble growth *via* rectified diffusion and other mechanisms.[11]

The ability of allylhydrazine to detect ROS was investigated *in vivo* using a LPS model of inflammation. Studies where microbubbles were taken up by cultured neutrophils and gas bubbles observed inside the cells have been reported.[15,16] The liver was chosen as the location for ROS imaging, because it is a major source of ROS production in the body; there is low ultrasound background signal; and the ease of identification during *in vivo* imaging. Our *in vivo* studies demonstrate that allylhydrazine can image oxidative stress in the mouse liver with good contrast and excellent spatial resolution (Fig. 4), on a timescale suitable for clinical applications (10 min). Allylhydrazine was encapsulated inside phospholipid liposomes to enhance delivery to the liver and to improve bubble stability. Both *in vitro* acoustic characterization and *in vivo* biodistribution studies confirmed that APLs are more effective at detecting ROS (Figs. 3a and 3d). Since the *in vivo* conditions inside the mouse liver are much more dynamic and complex, the exact ROS concentration *in vivo* cannot be quantified definitively without more advanced image processing techniques. In addition, allylhydrazine has known toxicity issues with an LD50 between 8300 and 9800 mg kg^{-1} orally in mouse.[37] There is therefore a potential for allylhydrazine in liposomes to have toxicity, and we anticipate that this potential toxicity can be mitigated by effective targeting of allylhydrazine to diseased tissues. However, given the clinical importance of oxidative stress, this work offers a potential new approach to address this problem.

CONCLUSIONS

The development of contrast agents that can image disease biomarkers in a clinical setting remains a major challenge. Ultrasound contrast agents have tremendous diagnostic potential because of their excellent contrast resolution and the widespread clinical use of ultrasound. Here, we demonstrate a new strategy for performing molecular imaging by ultrasound based on chemical reactions that generate gas forming molecules. This approach was demonstrated with the imaging of ROS by an allylhydrazine-based contrast agent, termed the APLs. The overproduction of radical oxidants is associated with many inflammatory diseases, and therefore the APLs have numerous potential applications. Moreover, numerous biologically important molecules, such as enzymes, thiols,[40] and the hydronium ion (pH)[33] participate in chemical reactions that generate gas forming molecules, and can potentially be imaged *via* ultrasound.

ACKNOWLEDGMENTS

This work was supported by NIH UO1 HL80711-01, (N.M.), NSF-BES-0546962 (N.M.), NIH U01 268 201000043C-0-0-1 (N.M.) and NIH RO1, HL096796-01 (N.M.), NIHR01CA112356 (K.F.) and NIHCA103828 (K.F.). The authors would like to thank Dr. Lihong Cheng for assisting the setup for the clinical ultrasound system.

REFERENCES

[1]Apfel, R. E., and C. K. Holland. Gauging the likelihood of cavitation from short-pulse, low-duty cycle diagnostic ultrasound. *Ultrasound Med. Biol.* 17(2):179–185, 1991.
[2]Barnham, K. J., C. L. Masters, and A. I. Bush. Neurodegenerative diseases and oxidative stress. *Nat. Rev. Drug Discov.* 3(3):205–214, 2004.
[3]Bird, R. B., W. E. Stewart, and E. N. Lightfoot. Transport Phenomena. New York: John Wiley, 2002.
[4]Blander, M., and J. L. Katz. Bubble nucleation in liquids. *AIChE J.* 21(5):833–848, 1975.
[5]Borden, M. A., and M. L. Longo. Dissolution behavior of lipid monolayer-coated, air-filled microbubbles: effect of lipid hydrophobic chain length. *Langmuir* 18(24):9225–9233, 2002.
[6]Bowers, P. G., K. Bar-Eli, and R. M. Noyes. Chemical oscillations and instabilities .100. Unstable supersaturated solutions of gases in liquids and nucleation theory. *Transactions* 92(16):2843–2849, 1996.
[7]Cable, M., and J. R. Frade. The influence of surface-tension on the diffusion-controlled growth or dissolution of spherical gas-bubbles. *Proceedings of the Royal Society of London Series A-Mathematical Physical and Engineering Sciences* 420(1859):247–265, 1988.
[8]Cadenas, E., and K. J. A. Davies. Mitochondrial free radical generation, oxidative stress, and aging. *Free Radical Biol. Med.* 29(3–4):222–230, 2000.
[9]Calderwood, T. S., C. L. Johlman, J. L. Roberts, C. L. Wilkins, and D. T. Sawyer. Oxidation of substituted hydrazines by superoxide ion—the initiation step for the autoxidation of 1,2-diphenylhydrazine. *J. Am. Chem. Soc.* 106(17):4683–4687, 1984.
[10]Chen, W. T., C. H. Tung, and R. Weissleder. Imaging reactive oxygen species in arthritis. *Mol. Imaging* 3(3):159–162, 2004.
[11]Chomas, J. E., P. Dayton, J. Allen, K. Morgan, and K. W. Ferrara. Mechanisms of contrast agent destruction. *IEEE Trans. Ultrason. Ferroelectr. Freq. Control* 48(1):232–248, 2001.
[12]Christiansen, J. P., H. Leong-Poi, A. L. Klibanov, S. Kaul, and J. R. Lindner. Noninvasive imaging of myocardial reperfusion injury using leukocyte-targeted contrast echocardiography. *Circulation* 105(15):1764–1767, 2002.

[13]Church, C. C. Spontaneous homogeneous nucleation, inertial cavitation and the safety of diagnostic ultrasound. *Ultrasound Med. Biol.* 28(10):1349–1364, 2002.
[14]Corey, E. J., G. Wess, Y. B. Xiang, and A. K. Singh. Stereospecific total synthesis of (+/−)-cafestol. *J. Am. Chem. Soc.* 109(15):4717–4718, 1987.
[15]Dayton, P. A., J. E. Chomas, A. F. H. Lum, J. S. Allen, J. R. Lindner, S. I. Simon, *et al.* Optical and acoustical dynamics of microbubble contrast agents inside neutrophils. *Biophys. J.* 80(3):1547–1556, 2001.
[16]Dayton, P. A., K. E. Morgan, A. L. Klibanov, G. H. Brandenburger, and K. W. Ferrara. Optical and acoustical observations of the effects of ultrasound on contrast agents. *IEEE Trans. Ultrason. Ferroelectr. Freq. Control* 46(1):220–232, 1999.
[17]Ferrell, R. T., and D. M. Himmelbl. Diffusion coefficients of nitrogen and oxygen in water. *J. Chem. Eng. Data* 12(1):111, 1967.
[18]Finkel, T., and N. J. Holbrook. Oxidants, oxidative stress and the biology of ageing. *Nature* 408(6809):239–247, 2000.
[19]Finkelstein, Y., and A. Tamir. Formation of gas-bubbles in supersaturated solutions of gases in water. *AIChE J.* 31(9):1409–1419, 1985.
[20]Forstermann, U. Oxidative stress in vascular disease: causes, defense mechanisms and potential therapies. *Nat. Clin. Pract. Cardiovasc. Med.* 5(6):338–349, 2008.
[21]Gomes, A., E. Fernandes, and J. L. F. C. Lima. Fluorescence probes used for detection of reactive oxygen species. *J. Biochem. Biophys. Methods* 65(2–3):45–80, 2005.
[22]Huang, S. L., and R. C. MacDonald. Acoustically active liposomes for drug encapsulation and ultrasound-triggered release. *Biochim. Biophys. Acta Biomembr.* 1665(1–2):134–141, 2004.
[23]Jabbari, A., E. J. Sorensen, and K. N. Houk. Transition states of the retro-ene reactions of allylic diazenes. *Org. Lett.* 8(14):3105–3107, 2006.
[24]Jones, S. F., G. M. Evans, and K. P. Galvin. Bubble nucleation from gas cavities—a review. *Adv. Colloid Interface* 80(1):27–50, 1999.
[25]Kakade, M. L., and I. E. Liener. Determination of available lysine in proteins. *Anal. Biochem.* 27(2):273–280, 1969.
[26]Lanza, G. M., and S. A. Wickline. Targeted ultrasonic contrast agents for molecular imaging and therapy. *Prog. Cardiovasc. Dis.* 44(1):13–31, 2001.
[27]Lasic, D. D. The mechanism of vesicle formation. *Biochem. J.* 256(1):1–11, 1988.
[28]Lee, D., S. Khaja, J. C. Velasquez-Castano, M. Dasari, C. Sun, J. Petros, W. R. Taylor, and N. Murthy. In vivo imaging of hydrogen peroxide with chemiluminescent nanoparticles. *Nat. Mater.* 6(10):765–769, 2007.
[29]Lee, J. C., H. Bermudez, B. M. Discher, M. A. Sheehan, Y. Y. Won, F. S. Bates, and D. E. Discher. Preparation, stability, and in vitro performance of vesicles made with diblock copolymers. *Biotechnol. Bioeng.* 73(2):135–145, 2001.
[30]Lindner, J. R., J. Song, F. Xu, A. L. Klibanov, K. Singbartl, K. Ley, and S. Kaul. Noninvasive ultrasound imaging of inflammation using microbubbles targeted to activated leukocytes. *Circulation* 102(22):2745–2750, 2000.
[31]Lubetkin, S. D. Why is it much easier to nucleate gas bubbles than theory predicts? *Langmuir* 19(7):2575–2587, 2003.
[32]Price, J. D., and R. P. Johnson. Thermal rearrangements of cyclic allenes via retro-ene reactions. *Tetrahedron Lett.* 26(21):2499–2502, 1985.
[33]Re, R., N. Pellegrini, A. Proteggente, A. Pannala, M. Yang, and C. Rice-Evans. Antioxidant activity applying an improved ABTS radical cation decolorization assay. *Free Radical Biol. Med.* 26(9–10):1231–1237, 1999.
[34]Rubin, M. B., and R. M. Noyes. Chemical oscillations and instabilities .77. Measurements of critical supersaturation for homogeneous nucleation of bubbles. *J. Phys. Chem.* 91(15):4193–4198, 1987.
[35]Ryan, P. J., and D. L. Melchior. Liposomes containing gas for ultrasound detection. USPTO #4900540, USA, 1990.
[36]Sashidhar, R. B., A. K. Capoor, and D. Ramana. Quantitation of epsilon-amino group using amino-acids as reference-standards by trinitrobenzene sulfonic-acid—a simple spectrophotometric method for the estimation of hapten to carrier protein ratio. *J. Immunol. Methods* 167(1–2):121–127, 1994.
[37]Toth, B., and D. Nagel. Tumor induction study with allylhydrazine HCl in swiss mice. *Br. J. Cancer* 34(1):90–93, 1976.
[38]Unger, E. Liposomes as contrast agents for ultrasonic imaging and method for preparing the same. 5123414. USPTO, USA, 1992.
[39]Weller, G. E. R., M. K. K. Wong, R. A. Modzelewski, E. X. Lu, A. L. Klibanov, W. R. Wagner, and F. S. Villanueva. Ultrasonic imaging of tumor angiogenesis using contrast microbubbles targeted via the tumor-binding peptide arginine-arginine-leucine. *Cancer Res.* 65(2):533–539, 2005.
[40]Zalipsky, S., N. Mullah, C. Engbers, M. U. Hutchins, and R. Kiwan. Thiolytically cleavable dithiobenzyl urethane-linked polymer-protein conjugates as macromolecular prodrugs: reversible PEGylation of proteins. *Bioconjugate Chem.* 18(6):1869–1878, 2007.
[41]Zheng, Q., D. J. Durben, G. H. Wolf, and C. A. Angell. Liquid at large negative pressures—water at the homogenous nucleation limit. *Science* 254(5033):829–832, 1991.